

Chapter 1

The origin of IceCube's neutrinos: Cosmic ray accelerators embedded in star forming calorimeters

E. Waxman

*Particle physics and Astrophysics department,
Weizmann Inst. of Science, Rehovot 76100, Israel*

The IceCube collaboration reports a detection of extra-terrestrial neutrinos. The isotropy and flavor content of the signal, and the coincidence, within current uncertainties, of the 50 TeV to 2 PeV flux and the spectrum with the Waxman-Bahcall bound, suggest a cosmological origin of the neutrinos, related to the sources of ultra-high energy, $> 10^{10}$ GeV, cosmic-rays (UHECR). The most natural explanation of the UHECR and neutrino signals is that both are produced by the same population of cosmological sources, producing CRs (likely protons) at a similar rate, $E^2 d\dot{n}/dE \propto E^0$, over the [1 PeV, 10^{11} GeV] energy range, and residing in "calorimetric" environments, like galaxies with high star formation rate, in which $E/Z < 100$ PeV CRs lose much of their energy to pion production.

A tenfold increase in the effective mass of the detector at $\gtrsim 100$ TeV is required in order to significantly improve the accuracy of current measurements, to enable the detection of a few bright nearby starburst "calorimeters", and to open the possibility of identifying the CR sources embedded within the calorimeters, by associating neutrinos with photons accompanying transient events responsible for their generation. Source identification and a large neutrino sample may enable one to use astrophysical neutrinos to constrain new physics models.

1. Introduction

The sources and acceleration mechanism of cosmic-rays of different energies have not been reliably identified despite many decades of research.^{1,2} Particularly challenging to models are the observations of UHECRs, since most models cannot account for the highest observed particle energies.^{2,3} One of the main goals of the construction of high energy neutrino telescopes is to resolve the open questions associated with these long standing puzzles.^{3,4}

Assuming that UHECRs are charged nuclei accelerated electromagnetically to high energy in astrophysical objects, some fraction of their energy is expected to be converted to high energy neutrinos through the decay of charged pions produced by the interaction of cosmic-ray protons/nuclei with ambient gas and radiation. A detection of this neutrino signal may enable the identification of the sources and will provide qualitative new constraints on accelerator models. The upper bound

derived by Waxman & Bahcall (WB) on the neutrino intensity produced by the CR sources^{5,6} implies that a giga-ton neutrino telescope is required to detect the expected flux in the energy range of ~ 1 TeV to ~ 1 PeV, and that a much larger effective mass is required at higher energy (see fig. 1(a)).

In this chapter we explain the reasoning leading to the conclusion, that the extra-terrestrial flux of neutrinos detected by the giga-ton IceCube detector^{7,8} is produced by UHECR sources embedded in "calorimetric" environments, characteristic of the conditions in galaxies with high star formation rate. The derivation of the WB bound is described in § 2. The implications of IceCube's detection and the constraints it imposes on the sources of high energy neutrinos and CRs are described in § 3. The main conclusions, the main open questions and the prospects for progress in the study of CR sources using high energy neutrinos of astrophysical origin are described in § 4.

2. The Waxman-Bahcall bound

2.1. UHECR composition, production rate and spectrum

The composition of UHECRs is controversial, with air-shower data from the Fly's Eye, HiRes and Telescope Array observatories⁹⁻¹¹ suggesting a proton dominated composition and data from the Pierre Auger Observatory¹² suggesting a transition to heavier elements above 10^{10} GeV. Due to this discrepancy, and due to the experimental and theoretical uncertainties in the relevant high energy particle interaction cross sections used for modeling the shape of the air showers, it is impossible to draw a definite conclusion regarding composition based on air-shower data at this time (the anisotropy signal provides an indication for a proton dominated composition,¹³ but is so far detected with only a $\sim 2\sigma$ confidence level²).

The observed flux and spectrum of $E > 10^{10.2}$ GeV CRs is consistent with a cosmological distribution of cosmic-ray sources, producing protons at a rate¹⁴⁻¹⁶

$$Q_{\text{UHE}} \equiv (E_p^2 d\dot{n}_p/dE_p)_{z=0} = 0.5 \pm 0.15 \times 10^{44} \text{erg/Mpc}^3 \text{yr}. \quad (1)$$

The energy density of CRs (at different energies) is determined by the (energy dependent) CR production rate and energy loss time. The energy loss of protons is dominated at high energy by the production of pions in interaction with cosmic microwave background (CMB) photons.^{17,18} The rate estimate of eq. 1 is based on the direct measurement of UHECRs and on the well understood physics of proton-CMB interaction. It is therefore accurate (to $\sim 30\%$) as long as the composition is dominated by protons. Observations determine only the local, $z = 0$, proton production rate and spectrum, since the energy loss time of protons is much smaller than the Hubble time (e.g., $\sim 3 \times 10^8$ yr corresponding to a propagation distance of ~ 100 Mpc at 10^{11} GeV).

The observed UHECR spectrum is consistent with a "flat" proton generation spectrum, $d \log \dot{n} / d \log E \approx -2$ with equal energy produced per logarithmic CR

energy interval, modified by interaction with CMB photons. This supports a proton dominated composition, since a flat generation spectrum is observed in a wide range of astrophysical environments (e.g. CR protons in the Galaxy,^{19,20} electrons in supernova remnants^{19,20} and in γ -ray bursts²¹), and is a robust prediction of the best understood and most widely accepted model for particle acceleration in astrophysical objects- Fermi acceleration in collisionless shocks^{19,22,23} (although a first principles understanding of the process is not yet available).

If the composition is dominated by heavier nuclei up to iron (e.g. O, Si, Fe), the inferred energy generation rate at $10^{10.5}$ GeV would change by a factor of only a few. This is due to the fact that the energy loss distance of protons is not very different from that of heavy nuclei (due to photo-disintegration interactions with the infrared background).²⁴ However, the different energy dependence of the energy loss distances of heavy nuclei and protons, implies that for a heavy nuclei composition, a generation spectrum different from $E^2 d\dot{n}/dE \propto E^0$ or an ad-hoc energy dependent composition would be required to fit the observed spectrum.²⁴ We consider this as further evidence supporting the proton dominated flux hypothesis, which we adopt in what follows. We return to the possibility of heavy nuclei domination in § 3.2.

2.2. *The neutrino intensity limit*

The energy production rate, eq. 1, sets an upper bound to the neutrino intensity produced by sources, which are optically thin for high-energy nucleons to $p\gamma$ and $pp(n)$ interactions. For sources of this type, the energy generation rate of neutrinos can not exceed the energy generation rate implied by assuming that all the energy injected as high-energy protons (eq. 1) is converted to pions (via $p\gamma$ and $pp(n)$ interactions). The resulting all-flavor upper bound is^{5,6}

$$E_\nu^2 \Phi_{\text{WB, all flavor}} = 3.4 \times 10^{-8} \frac{\xi_z}{3} \left[\frac{(E_p^2 d\dot{n}_p/dE_p)_{z=0}}{0.5 \times 10^{44} \text{erg/Mpc}^3 \text{yr}} \right] \text{GeV/cm}^2 \text{sr}, \quad (2)$$

where ξ_z is (a dimensionless parameter) of order unity, which depends on the redshift evolution of $E_p^2 d\dot{n}_p/dE_p$. The value $\xi_z = 3$ is obtained for rapid redshift evolution, $\Phi(z) = (1+z)^3$ up to $z = 2$ and constant at higher z , corresponding approximately to that of the star-formation rate or AGN luminosity density evolution ($\xi_z = 0.6$ for no evolution). The numerical value (3.4) given in eq. 1 is obtained for equal production of charged and neutral pions, as would be the case for $p\gamma$ interactions dominated by the Δ resonance.⁵ For $p\gamma$ interactions at higher energy, or $pp(n)$ interactions, the charged to neutral pion ratio may be closer to 2:1, increasing the bound flux by $\approx 30\%$.

Fig. 1(a) illustrates that a giga-ton neutrino telescope is required to detect the expected flux in the energy range of ~ 1 TeV to ~ 1 PeV, and that a much larger effective mass is required at higher energy. For a proton dominated UHECR flux, the WB bound is expected to be saturated at $\sim 10^{10}$ GeV, since most of the UHECR

protons that have been produced over a Hubble time would have lost all their energy to pion production in interactions with the CMB photons.²⁵

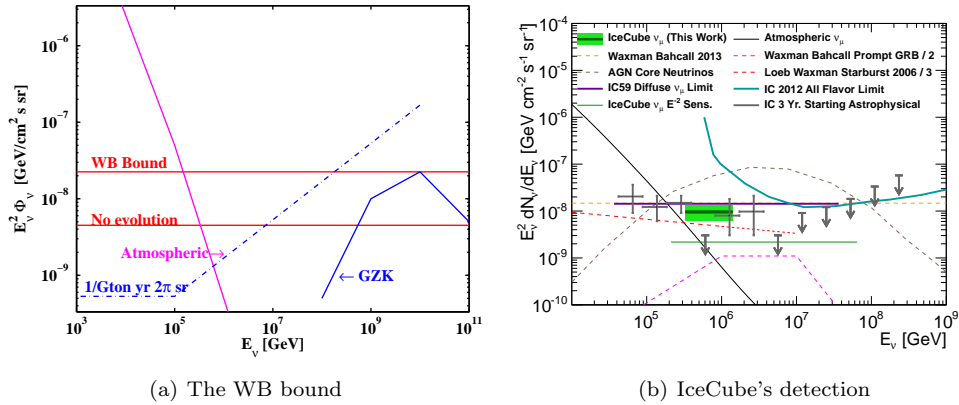


Fig. 1. (a) The upper bound imposed by UHECR observations on the extra-Galactic (all flavor) high energy neutrino intensity (lower-curve: no evolution of the energy production rate, upper curve: assuming evolution following the star formation rate), eq. 2, compared with the atmospheric neutrino background. The curve labelled "GZK" shows the neutrino intensity expected from UHECR proton interactions with micro-wave background photons.²⁵ The dash-dotted blue line shows the muon neutrino intensity that would produce one neutrino event per year in a detector with an effective mass of 1 Gton. (b) The extra-terrestrial neutrino signal (single flavor, assuming a $\nu_e : \nu_\mu : \nu_\tau = 1 : 1 : 1$ flavor ratio) detected by IceCube in the energy range of ~ 50 TeV to ~ 2 PeV (points with error bars "starting events" analysis;⁷ green shaded area- muon analysis;⁸ adopted from ref. 8). Within the current relatively large uncertainties, the detected extra-terrestrial signal coincides with the WB bound (eq. 2). Theoretical model predictions of the emission from particular astrophysical sources (starbursts,²⁶ GRBs,²⁷ AGNs²⁸) are also shown.

3. The origin of IceCube's neutrinos

3.1. The extra-terrestrial component of the neutrino flux

The IceCube collaboration reported⁷ a detection of 37 neutrinos in the energy range of ~ 50 TeV to ~ 2 PeV, which constitutes a 5.7σ excess above the expected atmospheric neutrino and muon backgrounds (the uncertain contribution of atmospheric neutrinos from charmed meson decay is constrained by the angular distribution of the detected events). The excess neutrino spectrum is consistent with a "flat", $E_\nu^2 dn_\nu/dE_\nu \propto E_\nu^0$, spectrum, its angular distribution is consistent with isotropy, and its flavor content is consistent with $\nu_e : \nu_\mu : \nu_\tau = 1 : 1 : 1$.²⁹ Assuming a flat spectrum, the best fit normalization of the intensity is $E_\nu^2 \Phi_\nu = (2.85 \pm 0.9) \times 10^{-8} \text{GeV/cm}^2 \text{s sr}$. Assuming that this intensity extends to high energy, 3 events should have been detected on average above 2 PeV. The absence of such events suggests a suppression of the flux above 2 PeV, or a softer than

$E_\nu^2 dn_\nu/dE_\nu \propto E_\nu^0$ spectrum. Fitting a power law excess, $dn_\nu/dE_\nu \propto E_\nu^{-\alpha}$ extending beyond 2 PeV, to the data yields $\alpha = 2.3 \pm 0.3$ (90% confidence).

The results of ref. 7 were obtained by an analysis limited to events for which the neutrino interaction occurs within the detector ("starting events"). A recent analysis⁸ searching for high energy neutrino induced muon events, not limited to neutrino interactions within the detector, revealed a muon-neutrino flux which constitutes a 3.7σ excess above the expected atmospheric neutrino and muon backgrounds in the energy range of ~ 300 TeV to ~ 1 PeV, with flux and spectrum consistent with those of the "starting events" analysis. The results of the "starting events" and muon analyses described above are shown graphically in fig. 1(b).

Extending the analysis to lower energy, ~ 10 TeV, where an astrophysical signal would be strongly dominated by the atmospheric flux, an excess of events is found at ~ 30 TeV³⁰ above an extension of the flat, $E_\nu^2 dn/dE_\nu \propto E_\nu^0$, > 50 TeV spectrum. This may indicate a new low energy component or a steeper ($\alpha \approx 2.5$) spectrum across the entire observed range. Robust conclusions cannot yet be drawn, since the significance of the excess is not high, 2σ ,³¹ and it is sensitive to the choice of energy bins (e.g. fig. 12 of ref. [30]). The possible low energy excess does not affect the analysis presented here, which is focused on the higher energy, > 50 TeV, neutrinos.

A $\nu_e : \nu_\mu : \nu_\tau = 1 : 1 : 1$ flavor ratio is consistent with that expected for pion decay in cosmologically distant sources, for which oscillations modify the original $1 : 2 : 0$ ratio to a $1 : 1 : 1$ ratio.³² However, with the current limited statistics, the data are consistent with any initial (i.e. at the source) flavor ratio.²⁹

3.2. UHECR sources in "cosmic calorimeters"

The extra-terrestrial neutrino flux is unlikely to be dominated by (yet unknown) Galactic sources, which, unlike the observed signal, are expected to be strongly concentrated along the Galactic disk. This, and the coincidence with the WB bound, suggests an extra-Galactic origin. IceCube's neutrinos are therefore most likely emitted by the decay of charged pions produced in interactions of high energy CRs with ambient (low energy) photons or protons in extra-Galactic sources.

Let us consider first the case where the parent CRs are protons. The fraction of the parent proton energy carried by each neutrino is approximately $1/20$ (for production by interaction with either photons or protons). Since the neutrino flux coincides with the bound given in eq. 2 over the ~ 50 TeV to ~ 2 PeV energy range, a lower limit of $E_p^2 d\dot{n}_p/dE_p \geq Q_{\text{UHE}}$ is implied on the local, $z = 0$, proton production rate in the energy range of ≈ 1 PeV to ≈ 50 PeV. Two distinct scenarios may be considered. The observed neutrinos may be produced by sources accelerating protons at a rate $E_p^2 d\dot{n}_p/dE_p \sim Q_{\text{UHE}}$, provided that protons of energy $E_p < 50$ PeV lose most of their energy to pion production either within the sources or at the sources' environment. Alternatively, the observed neutrinos may be produced by sources accelerating protons at a rate $(E_p^2 d\dot{n}_p/dE_p) \gg Q_{\text{UHE}}$, provided that protons lose only a small fraction, $f(E) \ll 1$, of their energy to pion production. In

the latter case, the small (and likely energy dependent) energy loss fraction $f(E)$ should compensate the large energy production rate, $(E_p^2 d\dot{n}_p/dE_p)/Q_{\text{UHE}} \gg 1$, to reproduce the observed flux and spectrum over two decades of ν energy, and the coincidence of the observed neutrino flux and spectrum with the WB bound would be an accident.

The simpler explanation, which we consider to be more likely, is that both the neutrinos and the UHECRs are produced by the same population of cosmological sources, producing protons with a flat spectrum, $d \log \dot{n}/d \log E \approx -2$ as observed in a wide range of astrophysics accelerators and as expected theoretically for electromagnetic acceleration in collisionless shocks (see § 2.1), over the [1 PeV, 10^{11} GeV] energy range, and residing in "calorimetric" environments, in which protons of energy $E_p < 50$ PeV lose much of their energy to pion production.

Let us consider next the case where the parent CRs are heavy nuclei of atomic mass A . The fraction of the parent nucleus energy carried by each neutrino emitted by the decay of charged pions produced in inelastic collisions with ambient protons is approximately $1/20A$, while interactions with ambient photons may lead to photo-disintegration of the nuclei, roughly preserving E/A . In this case therefore, a lower limit of $E_A^2 d\dot{n}_A/dE_A \geq Q_{\text{UHE}}$ is implied on the local, $z = 0$, production rate of nuclei in the energy range of $\approx 1A$ PeV to $\approx 50A$ PeV. As mentioned in § 2.1, if the UHECR flux is dominated by heavy nuclei, the energy production rate required to account for the observed UHECR flux would differ from that given by eq. 1 by a factor of a few at $10^{10.5}$ GeV. Thus, the observed neutrino flux and spectrum and the CR flux at $10^{10.5}$ eV could be explained by a single population of sources producing heavy nuclei with a flat spectrum, $d \log \dot{n}/d \log E \approx -2$ over the [1A PeV, 10^{11} GeV] energy range, and residing in "calorimetric" environments, in which nuclei of energy $E/A \approx E/2Z < 50$ PeV lose much of their energy to pion production.

Unlike the case of protons, if the UHECR flux is dominated by heavy nuclei, the $> 10^{10}$ GeV spectrum cannot be simply explained by an extension of a flat, $d \log \dot{n}/d \log E \approx -2$, spectrum to high energy (see § 2.1). We consider this an additional evidence supporting a proton dominated UHECR flux.

For all production channels, $p(A) - p(\gamma)$, similar flavor content (1 : 1 : 1) and particle/anti-particle content ($I_\nu = I_{\bar{\nu}}$) are expected, except for $p\gamma$ interactions dominated by the Δ resonance (which may be obtained in environments with soft, $d \log n_\gamma/d \log E_\gamma < -1$, photon spectra), where an excess of particles over anti-particles is expected.

Finally, we note that the absence of neutrino detection above a few PeV, which suggests a suppression of the neutrino flux above this energy, may be due to efficient escape of $E/Z > 100$ PeV CRs from the environments in which they produce the pions (as was predicted to be the case for sources residing in starburst galaxies²⁶), and need not imply a cutoff in the CR production spectrum (see § 3.3.1).

3.3. Star forming galaxies

3.3.1. Starburst calorimeters

Starburst galaxies have been predicted²⁶ to act as cosmic-calorimeters, producing an extra-Galactic neutrino background comparable to the WB bound at energies $E < 0.5$ PeV, and possibly extending to higher energy (see fig.1(b)). Starbursts may be defined as galaxies with specific star formation rate (sSFR), i.e. SFR per galaxy stellar mass, which is much higher than the average sSFR of galaxies at a similar redshift.³³ Starbursts in the local universe are characterized by disks of typical radii ℓ of several hundred parsecs, with column densities $\Sigma_g > 0.1 \text{g/cm}^2$ ³⁴⁻³⁶ and magnetic fields $B \sim 1 \text{mG}$ ($B \propto \Sigma_g$),³⁷ which are much larger than those of "normal" spiral galaxies ($\Sigma_g \approx 0.003 \text{g/cm}^2$, $B \sim 5 \mu\text{G}$ in the Milky way). The large disk densities imply that the energy loss time of CR protons, due to inelastic pp collisions, is much shorter in starburst galaxies than in normal spirals, and the enhanced magnetic field implies that the confinement time of the protons is expected to be larger than in normal spirals. This in turn implies that, unlike normal spirals, starburst galaxies may act as proton calorimeters.

Starburst galaxies have long been argued³⁴ to act as calorimeters for few GeV protons, based on the FIR-radio correlation. The recent detection of GeV and TeV emission from the nearby starburst galaxies M82 and NGC253 indicate that these galaxies are calorimetric for protons of energy exceeding 10 TeV.³⁸ The theoretical arguments given in ref. 26, and reproduced in a more general way below, suggest that calorimetry holds to energies exceeding 10 PeV.

Protons will lose all their energy to pion production provided that the energy loss time is shorter than both the starburst lifetime and the magnetic confinement time within the starburst gas. In the energy range of interest, the inelastic nuclear collision cross section is $\sigma_{pp} \approx 50 \text{mb}$, with inelasticity of ≈ 0.5 . The energy loss time, $\tau_{\text{loss}} \approx (0.5n\sigma_{pp}c)^{-1}$ where n is the interstellar nucleon density, would be shorter than the starburst lifetime, which is at least the dynamical time given by the ratio of ℓ to the characteristic gas velocities v , $\sim (2\ell/v)$, as long as

$$\Sigma_{\text{gas}} \gtrsim \Sigma_{\text{crit}} \equiv \frac{m_p v}{\sigma_{pp} c} = 0.03(v/300 \text{ km s}^{-1}) \text{ g cm}^{-2}. \quad (3)$$

For characteristic gas velocities, $v = \text{few hundred km/s}$, the critical surface density, Σ_{crit} , is comparable to the minimum Σ_{gas} of known starburst galaxies.^{34,37}

The ratio of confinement time and loss time is less straightforward to estimate, since magnetic confinement of CRs is not well understood. In the Milky Way, the total gas column density traversed by CRs of energy $E/Z \leq 1 \text{TeV}$ before they escape the Galaxy is $\Sigma_{\text{conf,MW}} \approx 9(E/10Z\text{GeV})^{-0.4} \text{g cm}^{-2}$.^{19,39} If the propagation of CRs in starburst galaxies is similar to that in our Galaxy, we may expect $\Sigma_{\text{conf,SB}}(E/Z) = (n_{\text{SB}}/n_{\text{MW}})\Sigma_{\text{conf,MW}}(B_{\text{MW}}E/B_{\text{SB}}Z)$, since the propagation of the CRs in the magnetic field is determined by E/ZB . For $n_{\text{SB}}/n_{\text{MW}} = B_{\text{SB}}/B_{\text{MW}} = 100$, the fraction of proton energy lost to pion production

before escape is $f_{\pi,SB} \approx 1(E/1\text{PeV})^{-0.4}$. Since the neutrino flux is expected to be dominated by starbursts at $z \gtrsim 1$, for which the typical surface density should be even higher than in local starbursts, it is reasonable to assume that most of the energy injected into starburst galaxies in $E \lesssim 10$ PeV protons is converted to pions.

3.3.2. *The fraction of CR production occurring in calorimetric galaxies*

The energy loss of $E \lesssim 10$ PeV protons in starburst galaxies would produce a neutrino flux and intensity similar to the WB bound at $E \lesssim 1$ PeV, provided that the sources of UHECRs produce most of their energy output in starburst environments. This would be the case if, as assumed in ref. 26, (i) the rate of CR production is proportional to the SFR and (ii) most (or a significant fraction) of the stars in the universe have been produced in starburst episodes.

The leading UHECR accelerator candidates are γ -ray bursts (GRBs) and transient accretion events onto massive black holes residing at the centers of galaxies.^{2,3} The assumption that the CR production rate is proportional to the SFR is natural for sources like GRBs, which are related to the deaths of massive stars, and may not be inconsistent with models based on activity around massive central black holes. On the other hand, the assumption that a significant fraction of the stars in the universe have been produced in starburst episodes (as suggested e.g. by ref. 40) is not necessarily valid.

Recent observations indicate that for $z < 2$ the sSFR is narrowly distributed around a z -dependent average, which increases by a factor of ~ 30 from $z = 0$ to $z = 2$.³³ Outliers with high sSFR, which may be categorized as starbursts, are found to contribute only $\sim 10\%$ of the total SFR.³³ The interpretation of these results is still debated. In particular, starburst activity has been commonly argued to be triggered by galaxy mergers, and whether or not the narrow distribution of the sSFR rules out major mergers as the cause for the rapid increase of the average sSFR with redshift is still debated.^{41,42} In other words, if starburst activity is driven by mergers and major mergers are responsible for the increase in the sSFR, all galaxies at higher redshift may be classified as starbursts.

While the definition of a starburst is debateable and the fraction of star-formation occurring in starburst episodes is still uncertain, it should be noted that the typical galaxies at high z , which are rapidly forming stars, may well be calorimetric. CO observations of 6 $z = 1.5$ galaxies with 'normal' (i.e. close to the average) sSFR show that they are characterized by rapid SFR, $\sim 100M_{\odot}/\text{yr}$, and high column density massive molecular disks, $\Sigma_g \sim 0.1\text{g}/\text{cm}^2$.⁴¹ In the local universe, galaxies with such column density and SFR are calorimetric(see eq. 3 and ref. 38). While the disk structure of high z galaxies may be different, and the determination of the high z molecular gas content is uncertain, these results support the hypothesis that a large fraction of the SFR occurred in calorimetric environments.

3.4. A lower limit to the density of steady sources

The non detection by IceCube of point sources producing multiple neutrino events, combined with the measured "diffuse" neutrino intensity, sets a lower limit to the density of the sources producing the neutrinos, and an upper limit to their neutrino luminosity. We give below a simple order of magnitude estimate of these limits.

Consider a population of "standard candle" sources, with density $n_s(z)$ and 0.1 to 1 PeV muon neutrino luminosity L_{ν_μ} . We consider only neutrino induced muon events, for which the arrival direction may be determined with good accuracy (better than 1 deg). The coincidence of the neutrino intensity with the WB bound implies, using eq. 2 and a measured 1 : 1 : 1 flavor ratio,

$$n_0 L_{\nu_\mu} \approx 2 \times 10^{43} \left(\frac{\xi_z}{3} \right)^{-1} \text{ erg/Mpc}^3 \text{ yr}, \quad (4)$$

where $n_0 \equiv n_s(z=0)$. The flux of neutrinos of energy E_ν required for the detection of more than one neutrino induced muon event is approximately given by $f_m = E_\nu / ATP_{\mu\nu}$, where A is the detector's effective area, T is the integration time, and the probability that a 1 TeV to 1 PeV neutrino with a propagation track crossing the detector would produce a muon going through the detector is $P_{\mu\nu} \approx 10^{-6} (E_\nu / 1 \text{ TeV})^4$. This yields $f_m \approx 2 \times 10^{-12} (AT / 3 \text{ km}^2 \text{ yr})^{-1} \text{ erg/cm}^2 \text{ s}$. The limit inferred below on n_0 implies that the distance d_m below which the flux exceeds f_m , $d_m = (L_{\nu_\mu} / 4\pi f_m)^{1/2}$, is $\ll c/H_0$. Thus, the number of sources producing multiple upward moving (and hence neutrino induced) muon events is approximately

$$N_m \approx \frac{2\pi}{3} n_0 d_m^3 \approx 1 \left(\frac{\xi_z}{3} \right)^{-3/2} \left(\frac{n_0}{10^{-7} \text{ Mpc}^{-3}} \right)^{-1/2} \left(\frac{A}{1 \text{ km}^2} \frac{T}{3 \text{ yr}} \right)^{3/2}. \quad (5)$$

The requirement $N_m < 1$ sets a lower limit to the density of steady sources, $n_0 > 10^{-7} \text{ Mpc}^{-3}$ (implying $L_{\nu_\mu} < 10^{43} \text{ erg/s}$ and $d_m < 200 \text{ Mpc}$), consistent with that of the detailed analysis of ref. 43. It rules out rare candidate sources, like bright $L \sim 10^{47} \text{ erg/s}$ AGN with $n_0 \sim 10^{-9} \text{ Mpc}^{-3}$, and is consistent with the density of starburst galaxies, $n_0 \sim 10^{-5} \text{ Mpc}^{-3}$.

4. Summary and discussion

4.1. The calorimetric star-forming galaxies model and its uncertainties

IceCube's measurements of extra-terrestrial neutrinos are consistent with a model in which both the neutrinos and the observed UHECRs are produced by the same population of cosmological sources, producing CR protons at a similar rate, $E^2 d\dot{n}/dE \propto E^0$, over the [1 PeV, 10^{11} GeV] energy range, and residing in "calorimetric" environments, in which $E < 50$ PeV protons lose much of their energy to pion production (§ 3.2). This model is a natural explanation of IceCube's results since it relies on a known (although not yet identified) population of sources- the

UHECR sources, and since it does not depend on ad-hoc choices or fine tuning of model parameters: the neutrino flux normalization is determined by the observed UHECR flux, and the neutrino spectrum is consistent with that implied by the measured UHECR spectrum (§ 2.1). Moreover, a "flat" $d \log \dot{n}/d \log E \approx -2$ generation spectrum is observed in a wide range of astrophysical environments^{19–21} and is a robust prediction of the most widely accepted and best understood (although not yet from first principles) model for particle acceleration in astrophysical objects—Fermi acceleration in collisionless shocks.^{19,22,23}

A wide variety of (non calorimetric) models for the neutrino origin were proposed following IceCube's discovery (including dark matter decay, active galactic nuclei of various types, see fig. 1(b), and galaxy clusters, see refs. 44,45 for reviews). These models generally rely on ad-hoc choices of model parameters, which cannot be derived theoretically or determined observationally, in order to reproduce the observed flux and spectrum of the neutrinos. Their predictive power is thus limited.

Radio to TeV observations of local starburst galaxies imply that they are calorimetric for protons of energy exceeding 10 TeV,^{34,38} and theoretical arguments suggest that calorimetry holds to energies exceeding 10 PeV (§ 3.3.1). Starburst galaxies have thus been predicted²⁶ (fig. 1(b)) to produce an extra-Galactic neutrino background comparable to the WB bound at energies $E < 0.5$ PeV, and possibly extending to higher energy, provided that (i) the rate of CR production is proportional to the SFR and (ii) most (or a significant fraction) of the stars in the universe have been produced in starburst environments. The validity of the first assumption is natural if UHECRs are produced by GRBs (and may hold also for models based on activity around massive central black holes). It is further supported by the observation that at low CR energy, ~ 10 GeV, the ratio of CR production rate to SFR is similar, $\sim 10^{47}$ erg for $1 M_{\odot}$ of star formation, in the Galaxy and in starburst galaxies, while their SFRs differ by orders of magnitude.⁴⁶

The production rate per unit volume of CR protons at ~ 10 GeV, $E^2 d\dot{n}/dE|_{10 \text{ GeV}}$, is only ~ 10 times the rate at UHE, suggesting that the same sources are responsible for the production of CRs of all energies,⁴⁶ from 1 GeV to 10^{11} GeV (implying $d \log \dot{n}/d \log E \simeq -2.1$). Alternatively, there may exist a population of sources, associated with star formation and embedded in starbursts (like supernovae), producing CRs at a rate and spectrum similar to that of the UHE sources but reaching only lower energy ($\ll 10^{10}$ GeV), and thus making a contribution to the lower energy CR flux and possibly to the 1 PeV neutrino flux,^{47–49} which is similar to that of the UHECR sources. In this scenario, the similarity of the energy production rates of the lower E and UHE sources requires an explanation^a.

The main uncertainty remaining is the fraction of stars formed in calorimetric environments. The observed neutrino intensity is dominated by sources at redshift 1–2. The 'average' galaxies at these redshifts produce stars at a much higher

^a The ad-hoc explanation given in the next to last parag. of ref. 26 is incorrect. It follows erroneous statements that are inconsistent with the rest of that article (That the local 1.4 GHz luminosity is dominated by starbursts, and that UHECRs do not escape starbursts)

rate than local galaxies,³³ and observations indicate that they are characterized by high column density molecular disks, $\Sigma_g \sim 0.1\text{g/cm}^2$.⁴¹ While this provides an indication that a significant fraction of the star formation occurred in calorimetric environments (§ 3.3), the structure of galaxy disks at this redshift range is poorly constrained.

The production of neutrinos by pion decay is accompanied by the production of high energy photons, which initiate electromagnetic cascades via interaction with infra-red background photons, leading to a background of $\lesssim 0.1$ TeV photons. In calorimetric models with a power-law proton spectrum, pion production by ~ 1 TeV protons contributes directly to the $\lesssim 0.1$ TeV photon background. The resulting background intensity is expected to contribute a significant fraction of the observed 0.1 TeV background,⁵¹ limiting the proton spectra to $d \log \dot{n}/d \log E > -2.2$.⁵²⁻⁵⁴

4.2. Open questions and the way towards their resolution

Due to the limited statistics and flavor discrimination power, the current uncertainties in the determination of the neutrino spectrum, angular distribution and flavor content are large (§ 3.1). A significant reduction of uncertainties requires a significant (order of magnitude) expansion of the effective mass of the detector at $\gtrsim 100$ TeV. Such expansion is necessary for example for a study of the hints for spectral breaks at low, < 30 TeV, and high, > 2 PeV energy, which are currently detected with low statistical significance. Reduced uncertainties will provide much more stringent constraints on predictive models, such as the calorimetric model.

An identification of the sources by angular correlation with a catalog of nearby sources is unlikely, since the fraction of events originating from $z < 0.1$ sources is $\approx 1/20$, implying that the fraction of well localized neutrino induced muon events from $z < 0.1$ sources over 2π sr is $\sim 1/200$.

A detection of neutrino emission from few nearby bright starburst galaxies would constitute a major evidence in support of the calorimetric star-forming galaxy model. Since the local density of starbursts is $n_0 \sim 10^{-5}\text{Mpc}^{-3}$, a ~ 10 -fold increase in the effective area of the detector at ~ 100 TeV is required in order to enable the detection of a few nearby sources (see eq. 5 and refs. 43,50).

An identification of the neutrino sources is likely to identify the calorimeters within which the CR accelerators reside, but not the accelerators themselves. The neutrino flux that is produced within the accelerators is expected to be significantly lower than the total neutrino flux produced in the calorimeters surrounding them. For example, if UHECRs are protons produced in GRBs, the neutrino flux expected to be produced within the GRB accelerators is $\approx 10\%$ ($\approx 1\%$) of the WB flux at 1 PeV (0.1 PeV)²⁷ (fig. 1(b)). Such a low flux would imply that had the accelerators been steady sources, even a tenfold increase in detector mass would have been unlikely to enable their identification. Luckily, the UHECR accelerators must be transient: The absence of (steady) sources with power output exceeding the minimum required for proton acceleration to 10^{11} GeV, $L > 10^{46}\text{erg/s}$, within

the ~ 100 Mpc propagation distance of such high energy protons, implies that the sources must be extremely bright transients.^{2,3} Their identification may be possible by an association of a neutrino with an electromagnetic signal accompanying the transient event. In order to open the possibility for such associations, a ten-fold increase in detector mass and a wide field electromagnetic transient monitoring program are required.

A large sample of high energy neutrinos may enable one to study both neutrino properties and possibly deviations from the standard model of particle physics (see ref. 45 for a recent summary of such possibilities). The identification of the sources is important for such studies, in order to discriminate between spectral/flux features originating from astrophysical and particle physics model effects (e.g. ref. 55).

Finally, while we have argued (§ 2.1, § 3.2) that a proton dominated composition is more likely, a heavy nuclei dominated composition cannot be excluded. A detection of (or stringent upper limit on) the GZK neutrino flux predicted for a proton dominated composition (§ 2.2, fig. 1(a)) will provide a clear confirmation of (or will rule out) a proton dominated composition. The recent analysis of Auger⁵⁶ sets an upper limit which is close to the WB bound at $\sim 10^{9.5}$ GeV, and the expected flux may be detectable by future radio experiments.^{57–59}

References

1. E. A. Helder, et al. *Space Sci. Rev.* **173**, 369–431 (Nov., 2012).
2. M. Lemoine, *Journal of Physics Conference Series.* **409**(1):012007 (Feb., 2013).
3. E. Waxman, in *Astronomy at the Frontiers of Science*, ed. J.-P. Lasota, Springer (Aug., 2011) (arXiv:1101.1155).
4. T. K. Gaisser, F. Halzen, and T. Stanev, *Phys. Rep.* **258**, 173–236 (July, 1995).
5. E. Waxman and J. Bahcall, *PRD.* **59**(2), 023002–+ (Jan., 1999).
6. J. Bahcall and E. Waxman, *PRD.* **64**(2), 023002–+ (July, 2001).
7. M. G. Aartsen, et al., *PRL.* **113**(10):101101 (Sept., 2014).
8. IceCube Collaboration, M. G. Aartsen, et al., arXiv:1507.04005 (July, 2015).
9. D. J. Bird, et al., *PRL.* **71**, 3401–3404 (Nov., 1993).
10. R. U. Abbasi et al. (HiRes Collaboration), *ApJ.* **622**, 910–926 (Apr., 2005).
11. R. U. Abbasi, et al., *Astroparticle Physics.* **64**, 49–62 (Apr., 2015).
12. A. Aab, et al., *PRD.* **90**(12):122006 (Dec., 2014).
13. M. Lemoine and E. Waxman, *JCAP.* **11**, 9–+ (Nov., 2009).
14. E. Waxman, *ApJ.* **452**, L1+ (Oct., 1995).
15. J. N. Bahcall and E. Waxman, *Physics Letters B.* **556**, 1–6 (Mar., 2003).
16. B. Katz, R. Budnik, and E. Waxman, *JCAP.* **3**, 20–+ (Mar., 2009).
17. K. Greisen, *PRL.* **16**, 748–750 (Apr., 1966).
18. G. T. Zatsepin and V. A. Kuz'min, *JETP Letters.* **4**, 78–+ (Aug., 1966).
19. R. Blandford and D. Eichler, *Phys. Rep.* **154**, 1–75 (Oct., 1987).
20. W. I. Axford, *ApJ Supp.* **90**, 937–944 (Feb., 1994).
21. E. Waxman, *Plasma Physics and Controlled Fusion.* **48**, B137–B151 (Dec., 2006).
22. J. Bednarz and M. Ostrowski, *PRL.* **80**, 3911–3914 (May, 1998).
23. U. Keshet and E. Waxman, *PRL.* **94**(11):111102 (Mar., 2005).
24. D. Allard, *Astroparticle Physics.* **39**, 33–43 (Dec., 2012).
25. V. S. Beresinsky and G. T. Zatsepin, *Physics Letters B.* **28**, 423–424 (Jan., 1969).

26. A. Loeb and E. Waxman, *JCAP*. **5**:003 (May, 2006).
27. E. Waxman and J. Bahcall, *PRL*. **78**, 2292–2295 (Mar., 1997).
28. F. W. Stecker, *PRD*. **72**(10):107301 (Nov., 2005).
29. M. G. Aartsen, et al., *PRL*. **114**(17):171102 (May, 2015).
30. M. G. Aartsen, et al., *PRD*. **91**(2):022001 (Jan., 2015).
31. M. G. Aartsen, et al., *ApJ*. **809**:98 (Aug., 2015).
32. J. G. Learned and S. Pakvasa, *Astroparticle Physics*. **3**, 267–274 (May, 1995).
33. M. T. Sargent, et al., *ApJ*. **747**:L31 (Mar., 2012).
34. H. J. Voelk, *A&A*. **218**, 67–70 (July, 1989).
35. J. J. Condon, et al., *ApJ*. **378**, 65–76 (Sept., 1991).
36. R. C. Kennicutt, Jr., *ApJ*. **498**, 541–552 (May, 1998).
37. T. A. Thompson, et al., *ApJ*. **645**, 186–198 (July, 2006).
38. B. C. Lacki, et al., *ApJ*. **734**:107 (June, 2011).
39. K. Blum, B. Katz, and E. Waxman, *PRL*. **111**(11):211101 (Nov., 2013).
40. S. Juneau, et al., *ApJ*. **619**, L135–L138 (Feb., 2005).
41. E. Daddi, et al., *ApJ*. **713**, 686–707 (Apr., 2010).
42. M. Puech, et al., *MNRAS*. **443**, L49–L53 (Sept., 2014).
43. M. Ahlers and F. Halzen, et al., *PRD*. **90**(4):043005 (Aug., 2014).
44. P. Mészáros, *Nuclear Physics B Proc. Supp.* **256**, 241–251 (Nov., 2014).
45. K. Murase. *AIP Conference Series*, **1666**, p. 040006 (July, 2015).
46. B. Katz, E. Waxman, T. Thompson, and A. Loeb, arXiv:1311.0287 (Nov. 2013).
47. H.-N. He, et al., *PRD*. **87**(6):063011 (Mar., 2013).
48. R.-Y. Liu, et al., *PRD*. **89**(8):083004 (Apr., 2014).
49. N. Senno, et al., *ApJ*. **806**:24 (June, 2015).
50. L. A. Anchordoqui, et al., *PRD*. **89**(12):127304 (June, 2014).
51. T. A. Thompson, E. Quataert, and E. Waxman, *ApJ*. **654**, 219–225 (Jan., 2007).
52. K. Murase, M. Ahlers, and B. C. Lacki, *PRD*. **88**(12):121301 (Dec., 2013).
53. X.-C. Chang and X.-Y. Wang, *ApJ*. **793**:131 (Oct., 2014).
54. I. Tamborra, S. Ando, and K. Murase, *JCAP*. **9**:043 (Sept., 2014).
55. T. Kashti and E. Waxman, *JCAP*. **5**, 6–+ (May, 2008).
56. A. Aab, et al., *PRD*. **91**(9):092008 (May, 2015).
57. P. W. Gorham, *Nuclear Physics B Proc. Supp.* **243**, 231–238 (Oct., 2013).
58. ARA Collaboration, P. Allison, et al., arXiv:1404.5285 (Apr. 2014).
59. S. W. Barwick, et al., *Astroparticle Physics*. **70**, 12–26 (Oct., 2015).